International Journal of Nanomedicine

Dovepress
open access to scientific and medical research

Open Access Full Text Article

ORIGINAL RESEARCH

Multicellular Spheroids Formation on Hydrogel Enhances Osteogenic/Odontogenic Differentiation of Dental Pulp Stem Cells Under Magnetic Nanoparticles Induction

Xiao Han[1,2]
Shijia Tang[1]
Lin Wang[1]
Xueqin Xu[2]
Ruhan Yan[2]
Sen Yan[3]
Zhaobin Guo[4]
Ke Hu[1,2]
Tingting Yu[5]
Mengping Li[2]
Yuqin Li[2]
Feimin Zhang[1,2]
Ning Gu[2,3]

[1]Jiangsu Key Laboratory of Oral Diseases, Affiliated Hospital of Stomatology, Nanjing Medical University, Nanjing, Jiangsu, People's Republic of China; [2]Laboratory of Oral Regenerative Medicine Technology, School of Biomedical Engineering and Informatics, Department of Biomedical Engineering, Nanjing Medical University, Nanjing, Jiangsu, People's Republic of China; [3]Jiangsu Key Laboratory for Biomaterials and Devices, School of Biological Science and Medical Engineering, Southeast University, Nanjing, Jiangsu, People's Republic of China; [4]Institute for Nanobiotechnology, Johns Hopkins University, Baltimore, MD, USA; [5]Department of Medical Genetics, School of Basic Medical Science & Jiangsu Key Laboratory of Xenotransplantation, Nanjing Medical University, Nanjing, Jiangsu, People's Republic of China

Correspondence: Feimin Zhang; Ning Gu
Fax +86-25-86516414; +86-25-83272460
Email fmzhang@njmu.edu.cn; guning@seu.edu.cn

Introduction: Promotion odontogenic differentiation of dental pulp stem cells (DPSCs) is essential for dentin regeneration. Physical cellular microenvironment is of critical importance for stem cells differentiation and influences the function of other biological/chemical factors to differentiation.

Methods: Based on adjusting the mechanical/interfacial properties of hydrogels, multicellular spheroids (MCSs) of DPSCs generated through self-organization. The spheroids were characterized by immunofluorescent staining and flow cytometry. Quantitative real-time polymerase chain reaction, alkaline phosphatase (ALP) activity assay, ALP staining and Alizarin Red S staining were performed to evaluate the osteogenic/odontogenic differentiation of DPSCs with or without magnetic iron oxide nanoparticles (IONPs) induction.

Results: MCSs of DPSCs exhibited a significant upregulation of E-cadherin and N-cadherin and enriched CD146 positive subpopulation, along with a stronger osteogenic/odontogenic differentiation ability. Moreover, DPSCs spheroids showed more substantial osteogenic differentiation tendency than the classical two-dimensional cultured DPSCs under the stimulation of magnetic IONPs.

Conclusion: Three-dimensional spheroids culture of DPSCs based on composite viscoelastic materials combined with mechanical/magnetic stimulation may provide a theoretical basis for the subsequent development of dentin or bone regeneration technology.

Keywords: tunable mechanical properties, dental pulp stem cells, magnetic nanomaterials, osteogenic/odontogenic differentiation, multicellular spheroids

Introduction

Dental caries, one of the most common oral diseases globally, is the main reason for dental hard tissues destruction and pulp exposure.[1–3] To preserve pulp vitality of deep lesion, pulp capping is currently the only available therapy, which is based on the formation of tertiary dentin by odontoblasts newly regenerated from dental pulp stem cells (DPSCs).[2] However, pulp capping is restricted in capping materials and few chosen cases.[4,5] Human DPSCs, first isolated from human extracted third molars by Gronthos et al in 2000, are postnatal stem cells with the ability of self-renewal and multipotent differentiation.[6] Notably, DPSCs are capable of differentiating into odontoblast-like cells and generating a dentin/pulp-like complex and thus a promising choice for dentin repair.[7,8] Therefore, a novel approach based on DPSCs for dentin regeneration is urgently needed.

Received: 6 May 2021
Accepted: 28 June 2021
Published: 27 July 2021

Mechanical properties of the cellular microenvironment, such as viscoelasticity of extracellular matrix (ECM), are thought to be distinguishing factors that regulate the fate of stem cells and could affect the cellular response to other biological/chemical factors.[4,9] Recent studies have reported that biomaterials with specific elasticity and tensile strength can promote osteogenic/odontogenic differentiation of DPSCs.[10,11] It was also found that three-dimensional (3D) spheroids culture of mouse dental papilla cells by anti-adhesive method could improve osteogenic/odontogenic differentiation.[12] However, conventional 3D culture methods, such as the hanging drop method, provide insufficient adhesion sites from environment and thus might triggering cell necrosis/apoptosis (e.g., anoikis), ultimately widening the gap between the experiments performed in vitro and in vivo.[13] Magnetic iron oxide nanoparticles (IONPs), the ferrimagnetic class of magnetic materials, applied independently or combined with scaffolds and magnetic fields promoted bone and dentin regeneration by delivering dynamic mechanical stimulation.[14–18] Recently, Cijun Shuai et al reported poly-L-lactide/polyglycolic acid scaffolds incorporated with IONPs significantly induced bone formation and vascularization in vivo and in vitro.[19] In addition, our group have found that magnetic IONPs have a significant promotion effect on osteogenic differentiation of stem cells in our preliminary research.[20] If the mechanical/interfacial properties of biomaterials for the DPSCs culturing can be adjusted to form multicellular spheroids (MCSs) while ensuring their cellular activity, it may be possible to promote the osteogenic/odontogenic differentiation ability of DSPCs under magnetic induction.

Hydrogels are promising biomaterials for ECM substitution, cell culturing and organ regeneration because of the excellent biocompatibility, and tunable mechanical properties.[21–23] Our previous works were focused on developing composite hydrogels platform as 3D culture substrates. By adjusting the composition of this platform, we designed specific mechanical microenvironments for a variety of cell types, such as fibroblasts, pancreatic β-cells and cancer cells, in order to promote those cells yielding unique biological output with respect to cellular function, signal transduction, as well as response to therapeutic intervention.[22,24–27] In this study, we designed two types of microenvironments for DPSCs with different mechanical properties based on the hydrogel platform to form monolayer cells (MLCs) or MCSs. In each condition, MLCs or MCSs formed as we expected, and cell morphology, viability, ECM molecules, surface markers and genes expression related to osteogenic/odontogenic differentiation were then examined with or without mechanical/magnetic stimulation of IONPs. Results demonstrated that DPSCs MCSs generated on hydrogels with controlled mechanical/interfacial properties were inclined to differentiate toward osteogenesis under stimulation of IONPs, which provides insights for the subsequent application of composite materials based on the design of cellular physical microenvironment combined with IONPs in dental restorations.

Materials and Methods

Preparation of the GelMA/PEGDA Composite Hydrogel

During the whole experiment, millipore water (18.25 MΩ cm^{-1}) prepared by Milli-Q Plus water system was used. Poly(ethylene glycol) diacrylate (PEGDA 2000 Mw) was purchased from Sigma-Aldrich Inc. GelMA with a substitution degree of 20% was purchased from Tissue Ink Co., Ltd. Lithium phenyl-2,4,6-trimethylbenzoylphosphinate (LAP) was purchased from StemEasy Inc. Unless otherwise stated, all other reagents were purchased from Aladdin Industrial Inc.

The hydrogels with different mechanical properties were prepared by adjusting the formula ratio. The preparation parameters and methods of the hydrogel were shown as followings: for hydrogels of culturing MCSs (Gel-MCSs), PEGDA (100 mg), N, N′-methylene-bis-acrylamide (0.3% wt.), and GelMA (50 mg) were added to 1 mL of water and dissolved at 50 °C for 2 h, while for culturing MLCs(Gel-MLCs), PEGDA (150 mg), N, N′-methylene-bis-acrylamide (0.3% wt.), and GelMA (50 mg) added. Then, LAP (5 mg) was added to the above mixture respectively and dissolved for 5 min. Then, the above-mentioned pre-cured gel solution was injected into a customized cylindrical mold (diameter: 2 cm; thickness: 1 mm) and irradiated under 405 nm visible light for 10 s to polymerize the GelMA/PEGDA hydrogel. The composite hydrogel was immersed in millipore quality water for 3 days and rinsed every 8 h. After sterilization with ethylene oxide, the hydrogel was used for cell culture.

Characterization of the Mechanical Properties of Hydrogels

The mechanical properties of hydrogels, mainly referring to stress relaxation time and Young's modulus, were

characterized by Piuma Nanoindenter (Optics11, Amsterdam, Netherlands). The optical probe of the Nanoindenter is spherical with a stiffness of 40.7 N/m and a tip radius of 24 μm. When measuring Young's modulus, the probe was set to press 10 μm in 2 s and unloaded after holding it for 1 s. When measuring the stress relaxation, the probe was set to press 15 μm in 5 s and unloaded after holding it for 600 s. During this process, the Piuma Nanoindenter's software was applied to collect the data of mechanical properties.

Primary DPSCs Isolation and Culture

Human DPSCs were isolated from the healthy third molars of 18- to 22-year-old patients which were extracted during the normal clinical treatment at the affiliated hospital of Stomatology, Nanjing Medical University. Informed consents were signed with the approval of the Ethics Committee of the affiliated hospital of Stomatology, Nanjing Medical University (permit number: PJ2019-068-001). After rinsing the tooth surfaces in phosphate-buffered saline (PBS), the pulp tissues were gently isolated and minced. Then the tissues were taken in the solution of 3 mg/mL of collagenase type I (Sigma-Aldrich, St. Louis, MO, USA) and digested for 20–30 min at 37°C. Cell suspension were seeded in culture dishes supplemented with Minimum Essential Medium α (MEM-α, Gibco; Thermo Fisher Scientific, Waltham, MA, USA) containing 20% fetal bovine serum (FBS, Gibco; Thermo Fisher Scientific, Waltham, MA, USA) and 2% penicillin/streptomycin (Gibco; Thermo Fisher Scientific, Waltham, MA, USA), in a humidified atmosphere of 5% CO_2 and 95% air. The medium was replaced every 3 days. DPSCs P4 was taken in the following experiments. The characterization of DPSCs was performed via multilinear differentiation and surface marker identification[28–30] and the results were shown in Figure S1.

Spheroids Formation and Monolayer Cells Culture of DPSCs on the Hydrogels

For the formation of MCSs or MLCs, DPSCs were seeded onto two different hydrogels at a density of 2×10^4 cells/cm^2 and 1×10^4 cells/cm^2 in basal MEM-α medium supplemented with 10% FBS and 1% penicillin/streptomycin, respectively. Traditional two-dimensional (2D) cell culture with dishes was also applied as a control. A fresh culture medium replacement was taken every 3 days. DPSCs spheroids or MLCs were applied in the following studies after 5 days of culture.

Time-Lapse Microscopy

At 5 days, cells on the hydrogels or dishes were imaged every 15 min at ×10 magnification for 24 h with an X-living cell workstation (Olympus, Tokyo, Japan).

Live/ Dead Staining

At 5 days of culture, the hydrogels with DPSCs spheroids or MLCs were transferred to confocal dishes and washed with PBS. Then DPSCs were stained using the LIVE/DEAD® Cell Imaging Kit (Invitrogen, Eugene, OR, USA). Cells were imaged with a laser scanning confocal microscope (LSM710; Zeiss, Jena, Germany) at a wavelength of 488 nm for living cells and 570 nm for dead cells.

Immunofluorescent Staining

DPSCs cultured on the hydrogels and dishes were rinsed with PBS, fixed in 4% paraformaldehyde for 15 min at room temperature (RT). Before immunofluorescence staining, fixed DPSCs were blocked using 3% BSA supplemented with 0.3% Triton X-100 for 30 min at RT. Then, cells were incubated for 2 h with primary antibody and washed twice with PBS. After secondary antibodies staining for 1 h at RT, nuclei were stained as the manufacturer's instruction (Invitrogen, Thermo Fisher Scientific, Waltham, MA, USA). Cell imaging was performed with a laser scanning confocal microscope (LSM710; Zeiss, Jena, Germany).

The primary and secondary antibodies in this examination mainly included as follows: rabbit anti-Collagen I antibody (Abcam, MA, USA), rabbit anti-Fibronectin antibody (Abcam, MA, USA), mouse anti-N Cadherin antibody (Abcam, MA, USA), mouse anti-E Cadherin antibody (Cell Signaling Technology, USA), Alexa Fluor 488 Donkey anti-Mouse IgG (Invitrogen, Eugene, OR, USA) and Alexa Fluor Plus 594 Donkey anti-Rabbit IgG (Invitrogen, Eugene, OR, USA).

Flow Cytometry Analysis

Single cells were collected with 0.25% trypsin-EDTA (Gibco, Thermo Fisher Scientific, Inc., Waltham, MA, USA) and then resuspended in cold PBS at a concentration of 5×10^6 cells/mL. Then, the cells were incubated in the dark on ice for 30 min using antibodies including anti-CD29, anti-CD34, anti-CD45, anti-CD73, anti-CD90, anti-CD105 and anti-CD146. All antibodies were purchased from BioLegend, Inc. Subsequently, cells

were twice washed and 500 μL PBS resuspension for each sample. The study was performed by Becton-Dickinson Accuri C6 (BD Biosciences, San Jose, CA, USA). FlowJo (version 10.0.7 r2) was used for the data analysis.

Quantitative Reverse Transcription–Polymerase Chain Reaction

After reaching 60% - 70% confluency, cells derived from spheroids or MLCs were cultured in human DPSCs osteogenic differentiation medium (Cyagen, Santa Clara, CA, USA). The total RNA of cells was extracted with RNAprep pure Cell/Bacteria Kit (Tiangen Biotech Co., Ltd., Beijing, China) at 7 days and 14 days of differentiation. cDNA was reversed-transcribed from 1 μg total RNA (Takara, Shiga, Japan). Quantitative reverse transcription–polymerase chain reaction (qRT-PCR) was performed using TB Green PCR Premix Ex Taq (Takara, Shiga, Japan) in the QuantStudio 7 Flex (Applied Biosystems, Foster City, CA, USA). The $2^{-\Delta\Delta Ct}$ method was used to evaluate the relative expression of genes. Primer sequences were listed in Table S1.

Alkaline Phosphatase Assay

At 7 and 14 days after osteogenic differentiation, alkaline phosphatase (ALP) activity kit (catalog no. A059-2, Jiancheng, Nanjing, China) and BCIP/NBT ALP Color Development Kit (catalog no. C3206, Beyotime, Shanghai, China) were applied to evaluate the ALP activity, which was normalized by total protein of each sample. The optical density was measured at 520 nm with a Multiskan Go Spectrophotometer (Spectramax M2e, Molecular Devices, San Jose, CA, USA).

Synthesis and Characterization of IONPs

The magnetic IONPs of γ-Fe_2O_3@PSC were synthesized according to the previous protocols.[31] To promote cellular uptake of IONPs, poly-L-lysine (PLL) was used to modify the γ-Fe_2O_3@PSC by mixing 10 g/mL PLL (Sigma-Aldrich, St. Louis, MO, USA) with 5 mg/mL γ-Fe_2O_3@PSC and sonicating for at least 3 h.

The morphology and hydrodynamic diameter of γ-Fe_2O_3@PSC and γ-Fe_2O_3@PSC /PLL were characterized by TEM (FEI Tecnai G2 F30, Hillsboro, USA) and dynamic light scattering (DLS) using a ζ-potential laser particle size analyzer (Litesizer 500, Anton Paar, Graz, Austria), respectively.

Prussian Blue (PB) Staining

γ-Fe_2O_3@PSC or γ-Fe_2O_3@PSC/PLL were added into the complete MEM-α medium with a concentration of 200 μg/mL, respectively. To reveal the cellular uptake of IONPs in MLCs and spheroids, PB staining was performed at 5 days of cell culture by a Prussian Blue Iron Stain Kit (Solarbio, Beijing, China). Cells derived from spheroids were also subjected to PB staining after seeding on the culture plates for 24 h.

Alizarin Red S (ARS) Staining

At day 21 days after differentiation, cells were fixed in 4% paraformaldehyde for 30 min at RT. Then, 1% alizarin red S solution (pH 4.2, Leagene, Beijing, China) was added. After incubation at RT for 5 min, cells were rinsed with PBS and imaged.

Statistical Analysis

Data are shown as mean ± SD acquired from at least three independent experiments. SPSS 25.0.0 (IBM Corp, Chicago, IL, USA) was used to analyze statistical significance. Student's *t*-test was performed for statistical comparison with a statistical significance level of $P < 0.05$.

Results

Tunable Mechanical Properties of Hydrogels for Monolayer and Multicellular Spheroids

Two types of hydrogels were fabricated by adjusting the formula ratio between GelMA and PEGDA (Figure 1A), and their mechanical properties represented by stress relaxation and Young's modulus, were first compared. The stress relaxation tests showed that the average half-relaxation time ($t_{1/2}$) of the hydrogel for Gel-MCSs group was ~ 2.13 s, confirming its more rapid stress relaxation than the hydrogel for MLCs with an average half-relaxation time ($t_{1/2}$) for ~155.06 s (Figures 1B–C). Similarly, Young's modulus of hydrogel for spheroids formation was 214.3 kPa, two-folds lower than the hydrogel for MLCs (Figures 1D–E). These results indicated the significant distinction of the mechanical properties between the two types of hydrogels, which might result in distinguished microenvironments for cells and modulate cellular fate further.

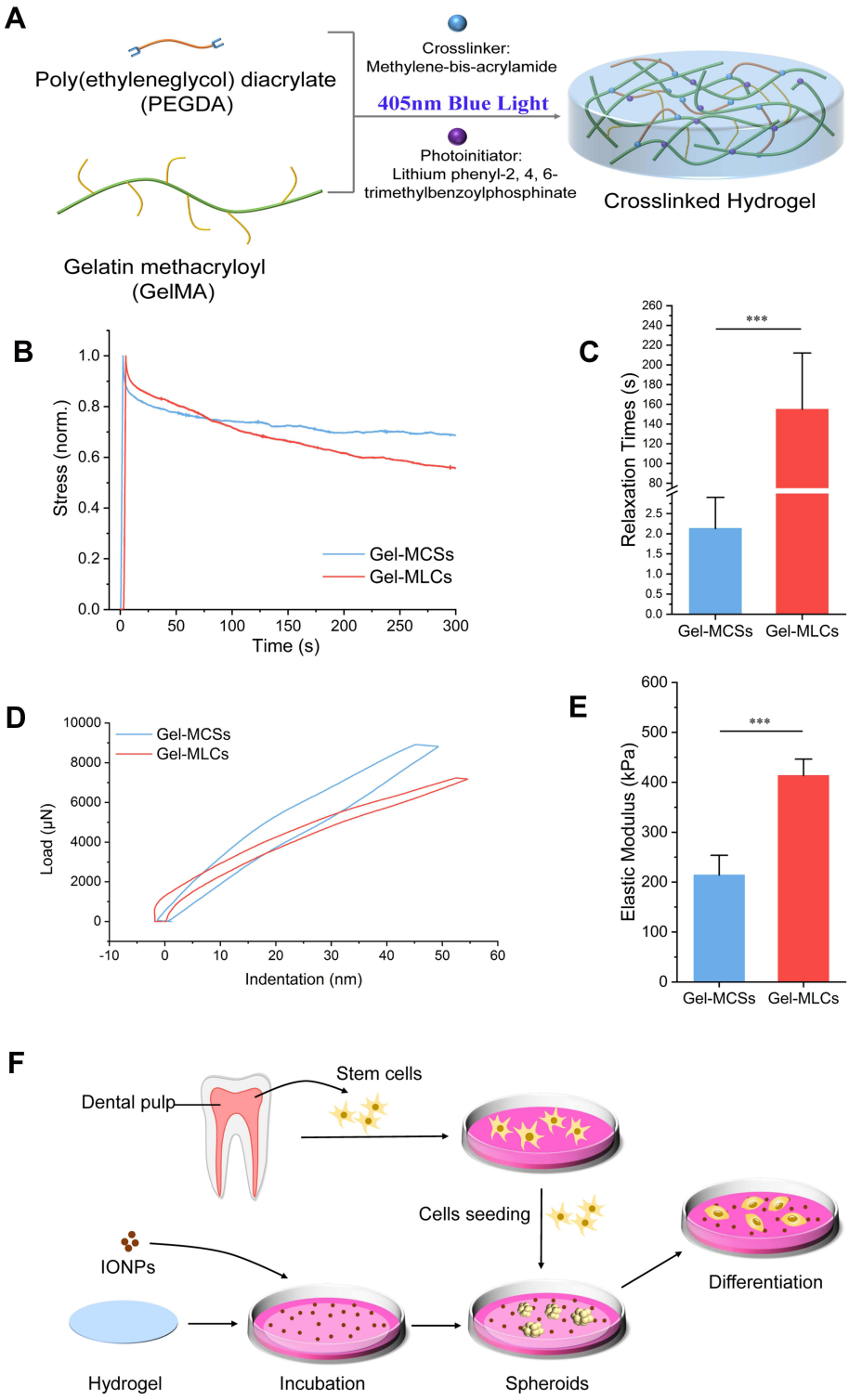

Figure 1 Preparation and characterization of the hydrogel and the schematic of DPSCs spheroids formation on the hydrogel with IONPs.(**A**) Schematic of the preparation of the GelMA/PEGDA composite hydrogel. Firstly, PEGDA and GelMA were mixed with N, N'-methylene-bis-acrylamide and LAP. Then the mixture was irradiated under 405 nm blue light to polymerize the hydrogel. Stress relaxation tests (**B, C**) and elasticity tests (**D, E**) of the 2 types of hydrogels. ***P<0.001(Student's t test). Data are shown as mean ± SD(n≥3). (**F**) Schematic of DPSCs spheroids formation on the hydrogel with IONPs.

Morphology and Viability of DPSCs Cultured on Hydrogels

Figure 1F showed the schematic of DPSCs isolation and spheroids formation process on the hydrogel. DPSCs were cultured on two types of hydrogels and conventional polystyrene cell-culture plates. At 24 h of culture, as we expected, cellular monolayer formed on polystyrene plates and 2D cell culture hydrogels, while spheroids formed on 3D cell culture hydrogel, respectively. In both hydrogel conditions, cells were well adhering on the substrates and no substantial apoptosis was observed (Figure 2B). We next performed the time-lapse images every 15 min at ×10 magnification for 24 h to visualization the process of MLCs and MCSs formation. As observed in images, cells on the 2D plates or 2D culture hydrogels spread, migrated, and proliferated, and cells on 3D culture hydrogels aggregated initially, then merged and compacted (Figure 2A).

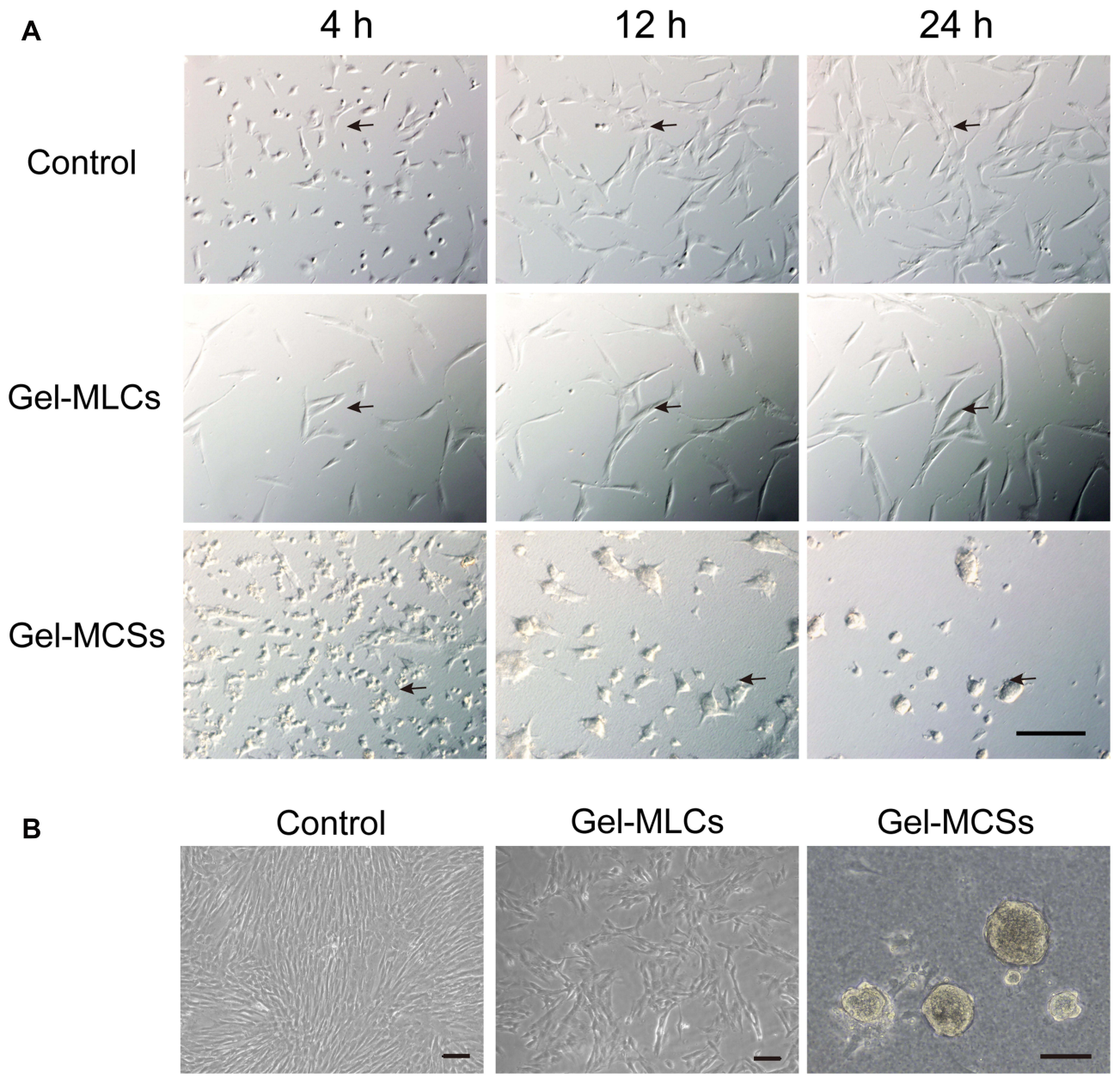

Figure 2 DPSCs motility and morphology of monolayer cells and spheroids. (**A**) Time-lapse microscope images of DPSCs cultured on cell-culture plates and hydrogels lasting for nearly 24 h after seeding. Arrows indicate the formation process of monolayer and spheroids by migration, proliferation and mergence. Scale bar : 200 μm. (**B**) Morphology of DPSCs after 1 day culture. Scale bar: 100 μm.

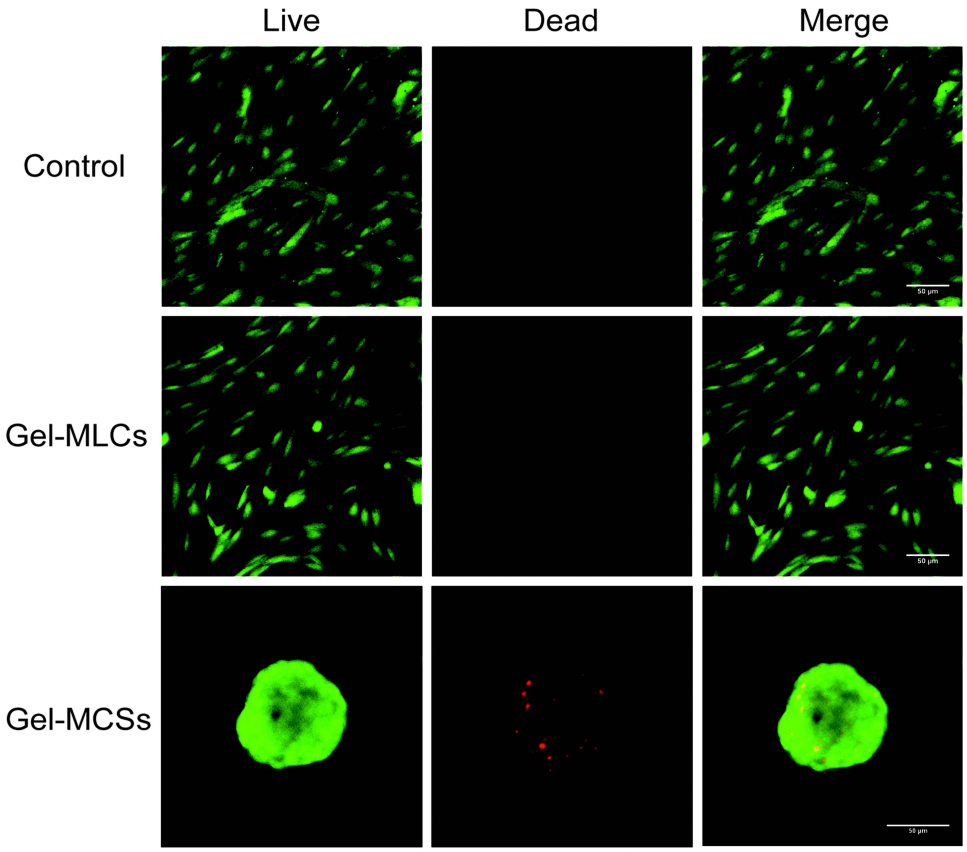

Figure 3 DPSCs viability of monolayer cells and spheroids. At 5 days, DPSCs cultured on cell-culture plates and hydrogels for Gel-MLCs and Gel-MCSs were subjected to live/dead staining. Live: green, dead: red. Scale bar: 50 μm.

After 5 days of culture, live/ dead staining was performed to evaluate the viability of DPSCs in 3 groups. No substantial cell death was observed when cells cultured on the plates or 2D culture hydrogels. A small number of dead cells were found in the core of spheroids on the 3D culture hydrogels (Figure 3). This is expected and reported in the literature that some cells in the central region of well formed MCSs were of lower viability compared to those in the peripheral regions, which due to the barrier functions formed in the periphery that limited the accessibility of nutrients and oxygen by cells in central region from environment.[13]

Fibronectin (FN), Collagen I (Col-I), E- and N-Cadherin (E-Cad and N-Cad) Expressions in DPSCs by Immunofluorescence Staining

FN, Col-I, E- and N-cad are proteins expressing on cell membrane and play important roles in mediating cell–cell/cell–matrix interaction. Thus, we evaluated the expression of these four proteins by immunofluorescence staining at 5 days of culture. Higher expression of E- and N-cad were found in Gel-MCSs group than the control and Gel-MLC s group, in which E- and N-cad were rarely observed. FN and Col-I were found expressing in each condition (Figure 4). The results indicated the upregulation of E- and N-cad in response to mechanical microenvironmental stimuli might be one of the upstream regulators of spheroids formation, considering the prominent role of E- and N-cad in the process of spheroids formation.

Expression of Pluripotency and Surface Markers of DPSCs

The mRNA expression levels of pluripotency markers, including Nanog, OCT4 and SOX2 genes, were also evaluated at 5 days of culture. The Gel-MCSs group exhibited significantly higher expressions of Nanog, OCT4 and SOX2 than the control and Gel-MLCs group, while no significant differences were found between the control and

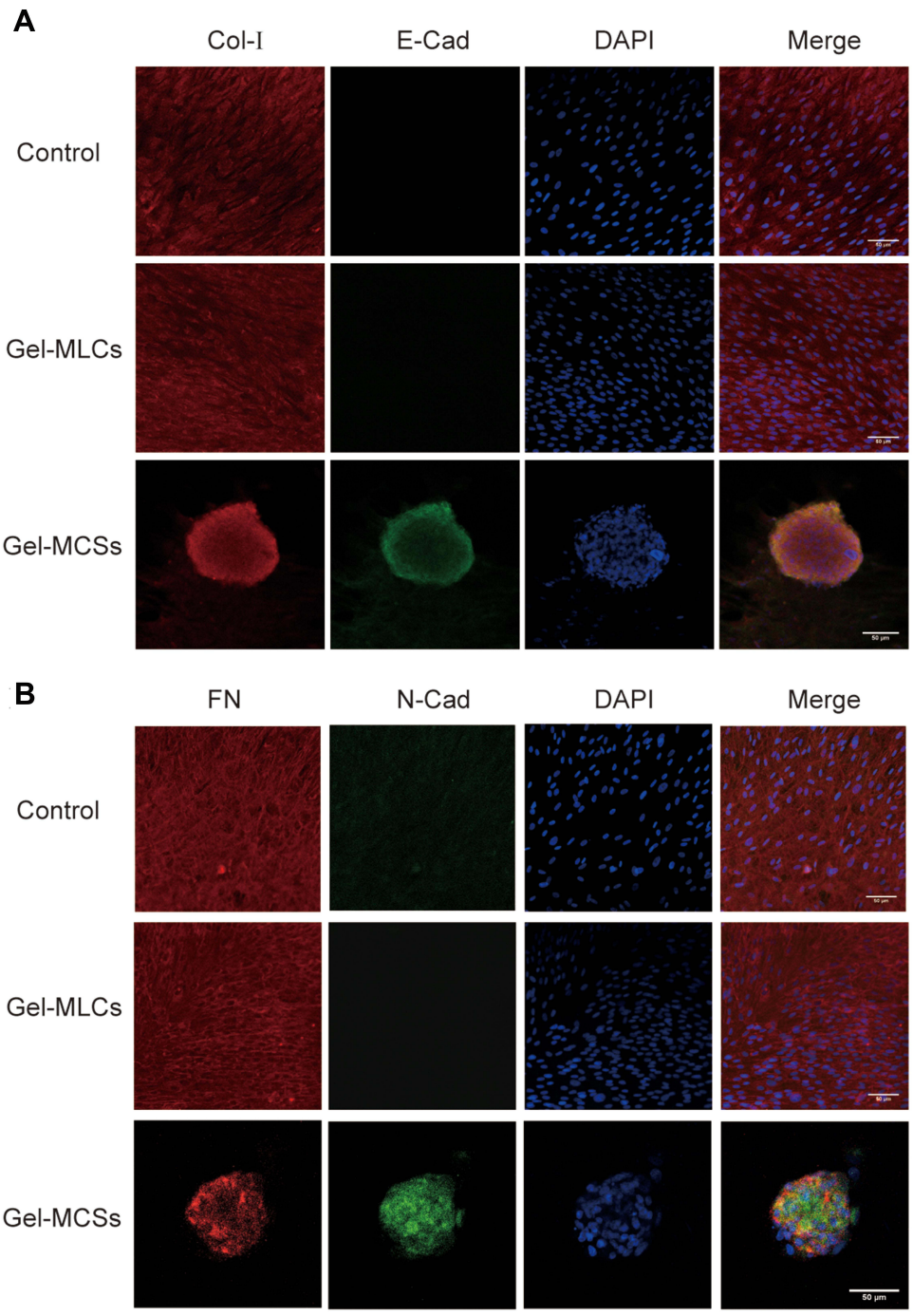

Figure 4 Expression of the ECM related molecules. At 5 days, ECM related molecules of DPSCs from the cell-culture plates and hydrogels of Gel-MLCs and Gel-MCSs, including Col-I and E-cad (**A**), FN and N-cad (**B**), were evaluated by immunofluorescence staining. Scale bar: 50 μm.

the Gel-MLCs group. These results suggested cells maintained on the 3D culture hydrogels acquired better self-renew properties compared to the other conditions (Figure 5A). Raw data see Table S2.

To characterize the immunophenotype difference, stem cell surface antigens were examined by flow cytometry at day 5. Cells from each group had high percentages of positive CD29, CD73, CD90 and CD105 expression, and extremely low percentages of CD34 and CD45. These results indicated that DPSCs maintained their specific immunophenotypes under 2D/3D culture systems on the hydrogels (Figure S2). Notably, the number of $CD146^{+}$cells from

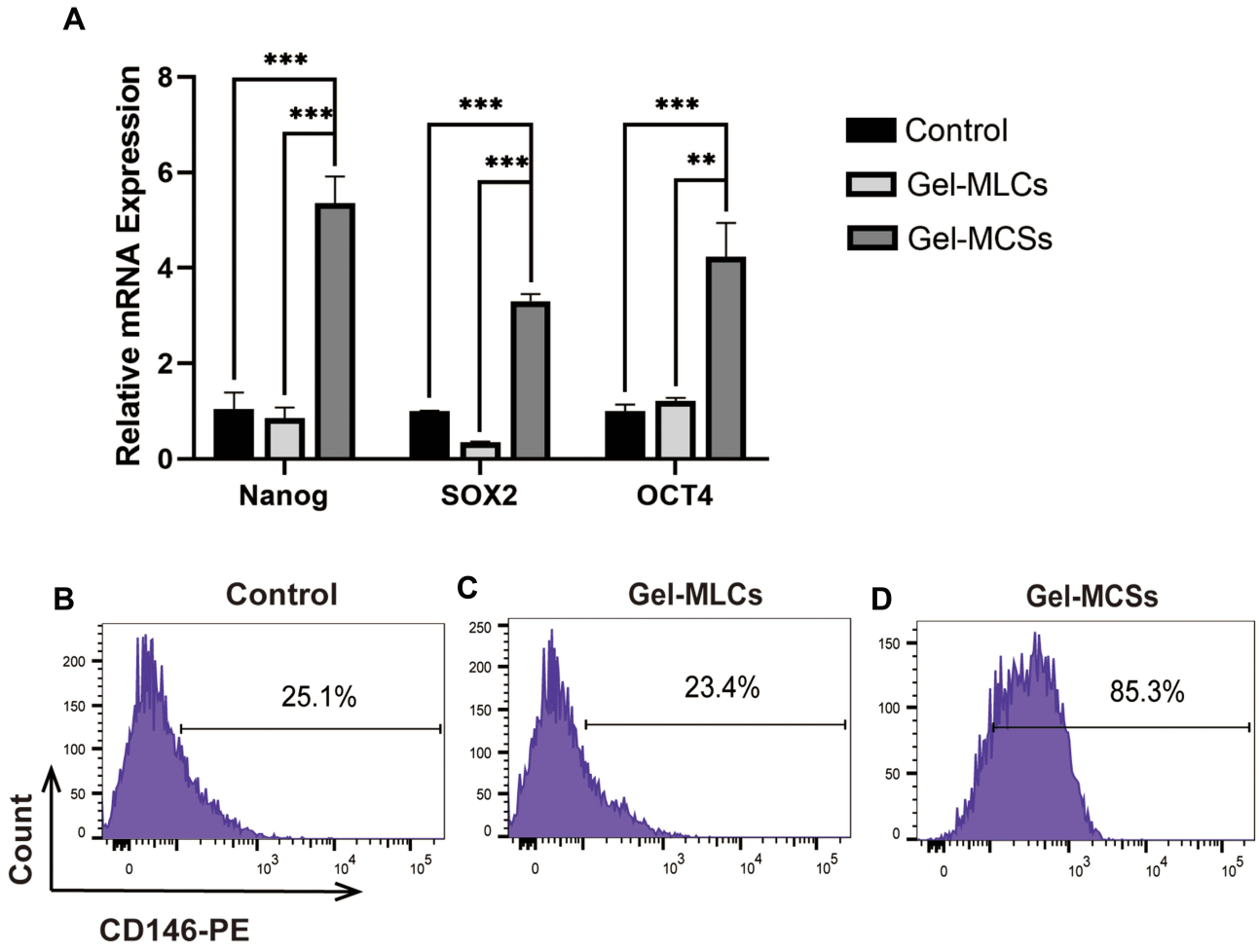

Figure 5 mRNA expression of pluripotency markers and the flow cytometry results of CD146$^+$ subpopulation. (**A**) Relative mRNA expression of pluripotency markers, including Nanog, SOX2 and OCT4, at 5 days culture on cell-culture plates and hydrogels. **P<0.01, ***P<0.001 (Student's t test). Data are shown as mean ± SD(n≥3). (**B-D**) CD146, a cell adhesion molecule, was detected by flow cytometry. Other surface markers for stem cells (CD29, CD34, CD45, CD73, CD90, CD105) were also evaluated (**Figure S2**).

spheroids was strikingly higher compared to the control and Gel-MLCs, suggesting the CD146$^+$ cells were enriched on 3D cell culture hydrogels (Figures 5B-D).

Osteogenic/Odontogenic Differentiation of DPSCs

To evaluate the osteogenic/odontogenic differentiation capacity of DPSCs, cells were cultured in osteogenic differentiation medium. After 7 days and 14 days of induction, DPSCs deprived from spheroids expressed the highest levels of osteogenic/odontogenic related genes, including ALP, runt-related transcription factor 2 (RUNX2), osteocalcin (OCN), bone morphogenetic protein 2 (BMP2), dentin sialophosphoprotein (DSPP), compared to cells from 2D plates and 2D culture hydrogels (Figures 6A–B). Raw data see Tables S3 and Table S4.

ALP activity measurement was also performed at day 7 and 14. While the ALP activity of Gel-MLCs group was slightly decreased compared to the control, it was significantly elevated in the Gel-MCSs group. Raw data are shown in Table S5. Similar results ALP staining for 7 days and ARS staining for 21 days were obtained (Figures 6C–D). These data demonstrated that the ability of osteogenic differentiation was strengthened for cells derived from DPSCs spheroids.

Characterization and Cellular Uptake of IONPs

TEM images revealed the uniformed particle size of γ-Fe_2O_3@PSC and γ-Fe_2O_3@PSC/PLL and their mean hydrodynamic diameter measured by DLS were ~38.45nm and ~246.16nm, respectively (Figures 7A–

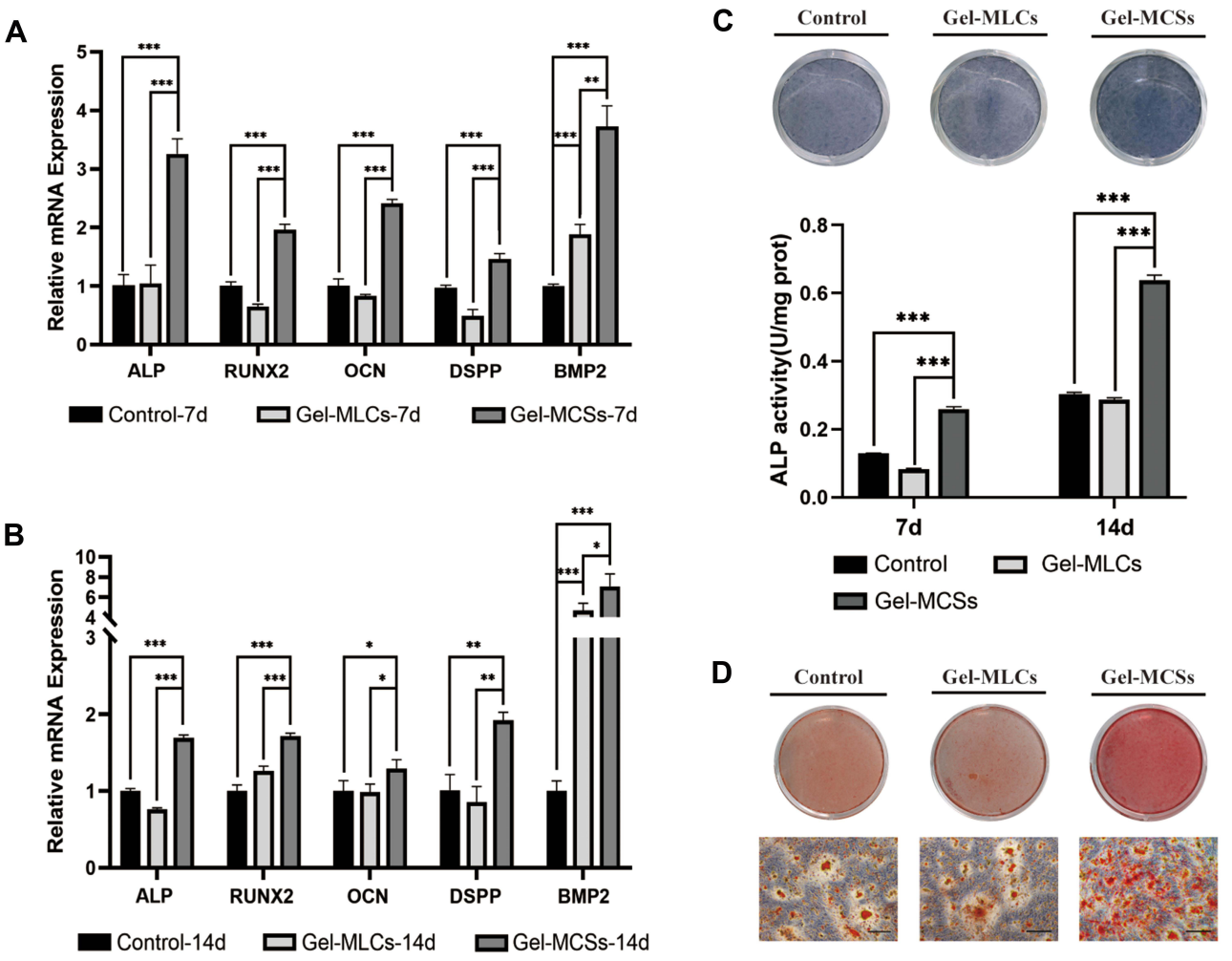

Figure 6 Osteogenic/odontogenic differentiation of DPSCs. The mRNA expression levels of osteogenic/odontogenic differentiation markers in different groups were measured at 7 days (**A**) and 14 days (**B**) of culturing in osteogenic differentiation medium, respectively. *P<0.05, **P<0.01 and ***P<0.001(Student's t test). Data are shown as mean ± SD(n≥3). (**C**) ALP staining at 7 days and ALP activity at day 7 and 14. ***P<0.001 (Student's t test). Data are shown as mean ± SD (n≥3). (**D**) Images of ARS staining at 21 days of induction. Scale bar: 200 μm.

B). PB staining of MLCs showed visibly intracytoplasmic blue particles in DPSCs with γ-Fe_2O_3@PSC/PLL nanoparticles in contrast to DPSCs with γ-Fe_2O_3@PSC nanoparticles. For MCSs, the PB staining image for DPSCs with γ-Fe_2O_3@PSC nanoparticles revealed that blue particles only located in the spheroids core, whereas royal blue suffused the whole spheroids with γ-Fe_2O_3@PSC/PLL (Figure 7C). The results demonstrated it was γ-Fe_2O_3@PSC/PLL, rather than γ-Fe_2O_3 @PSC, uptake by DPSCs. This was further confirmed by PB staining of cells derived from spheroids in 2D cell culture. Moreover, it also indicated that a number of γ-Fe_2O_3@PSC nanoparticles were encapsulated in the spheroids without cellular uptake during the process of their generation.

The Influence of IONPs on Osteogenic Differentiation of DPSCs

To evaluate the influence of IONPs on osteogenic differentiation of DPSCs, genes expression of osteogenic markers at 7 and 14 days induction were analyzed. The expression of RUNX2, OCN and BMP2 was significantly increased in MLCs with γ-Fe_2O_3@PSC/PLL, compared to MLCs with γ-Fe_2O_3@PSC. A similar tendency was also shown in cells from MCSs . Expression of ALP also upregulated, but the difference was significant only in MLCs (Figures 8A–B). Raw data see Tables S6 and Table S7. ALP activity of cells with γ-Fe_2O_3@PSC/PLL at 7 days was also elevated (Figure 8D). Raw data are shown in Table S8. Moreover, ALP staining at day 7 (Figure 8C) and ARS staining at day 21 (Figure 8E)

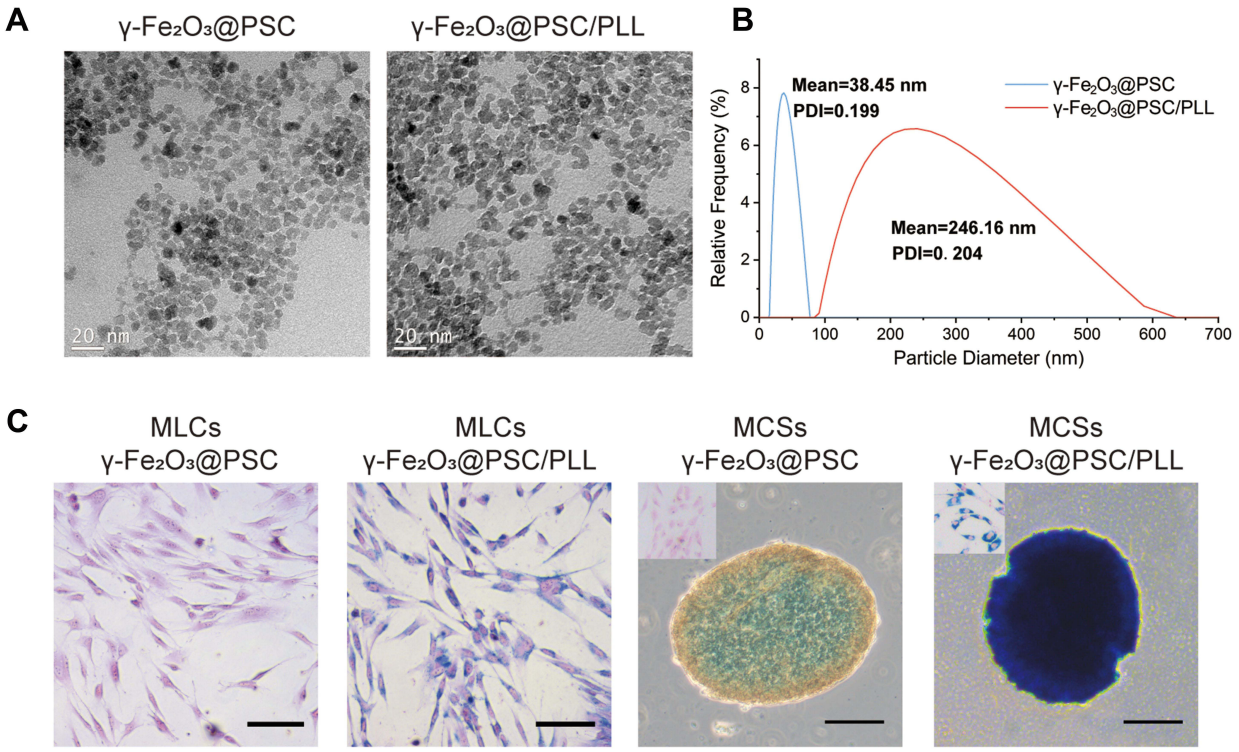

Figure 7 Characterization of IONPs and their cellular uptake. (**A-B**) Characterization of IONPs. Scale bar: 20 nm. (**C**) PB staining of MLCs and MCSs. Scale bar: 100 μm.

further confirmed an enhanced osteogenic differentiation with γ-Fe_2O_3@PSC/PLL both in MLCs and MCSs, which demonstrated the cellular uptake of IONPs played predominant roles in modulating stem cells fate.

Discussion

In the present study, 3D cell-culture platform for human DPSCs was established based on hydrogels with tunable mechanical properties by changing the ratio of GelMA and PEGDA, the main composition of the hydrogel platform. DPSCs spheroids generated by self-assembly on the hydrogels exhibited enhanced osteogenic/odontogenic differentiation with or without IONPs.

Stem cells are susceptible to mechanical cues, and cell fate can be regulated by cell–cell/cell–matrix interaction.[32,33] Compared to 2D cell culture, cell spheroids with differential cell–cell/cell–matrix interactions similarly to the in vivo, are pivotal materials for regenerative medicine.[34] Based on our previous studies, MCSs formation depended on the density and distribution of cell adhesive sites.[22,35] GelMA ratio not only affected the adhesion, but also altered the hydrogel mechanical properties.[24] We previously developed 3D culture systems for pancreatic β cells and cancer cells by adjusting mechanical properties of hydrogels.[22,24–26] Based on these results, culture platforms specifically for DPSCs monolayer and spheroids were established in this study. The shorter stress relaxation time and lower Young's modulus of hydrogel for spheroids formation indicated it was viscoelastic and soft, while the hydrogel was more elastic and rigid for MLCs formation, supported by longer stress relaxation time and higher Young's modulus. Viscoelasticity is an intrinsic property of natural ECM, which is particularly crucial for cell spreading, proliferation, differentiation, and organoid formation.[36–38] Thus, we speculated that the hydrogel of the Gel-MCSs group provided microenvironment for DPSCs that better mimic the ECM viscoelasticity in vivo compared to the 2D control and Gel-MLCs group.

The interactions of cell–cell/cell–matrix in 2D and 3D cell culture platform were next examined. E-cad and N-cad are two prominent transmembrane adhesion molecules and both of them are essential for solid tissues formation.[39] E-cad has been recognized as a primary molecule for aggregation of mesenchymal stem cells (MSCs) and its absence could lead to the transformation

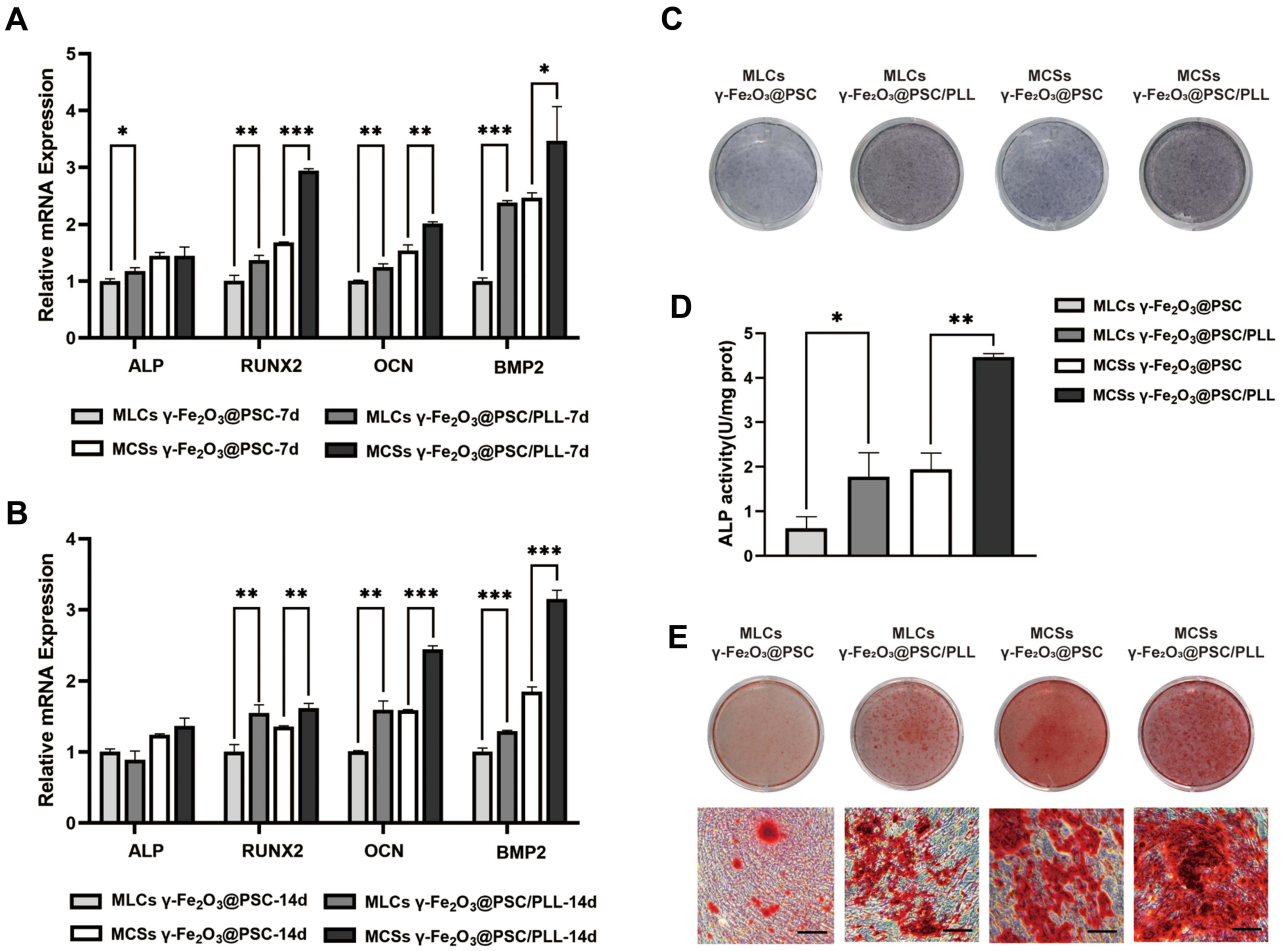

Figure 8 Effects of IONPs on osteogenic differentiation of DPSCs. The mRNA expression levels osteogenic differentiation markers were measured at 7 days (**A**) and 14 days (**B**) of culturing in osteogenic differentiation medium, respectively. *P<0.05, **P<0.01 and ***P<0.001 (Student's t test). Data are shown as mean ± SD (n≥3). (**C**) ALP staining at day 7. (**D**) ALP activity at 7 days. *P<0.05, **P<0.01 (Student's t test). Data are shown as mean ± SD(n≥3). (**E**) Images of ARS staining at 21 days of osteogenic differentiation induction. Scale bar: 200 μm.

of pluripotency related signal pathways.[40,41] Importantly, recent studies reported N-cad could regulate the mechanosensing ability of stem cells to microenvironment in addition to E-cad, which indicated its important functions on stem cells self-renew.[41,42] The immunofluorescence staining results in the present study were well consistent with that E-cad and N-cad promoted MCSs formation. FN and Col-I, structural constitutes of ECM, were observed in each group, which were different from our previous observation on pancreatic β-cells.[24] Mechanisms underlying this distinction is not clear, but likely due to the difference between cell types, which we believe warrants an in-depth investigation in the further studies.

CD146 is a transmembrane adhesion molecule belonging to the immunoglobulin superfamily. It plays an important role in the interactions of cell–cell/ cell–matrix and involved in cell cycle, cell migration, signaling transduction, stem cells self-renewal and angiogenesis.[43–45] The subpopulation of CD146 was reduced with the senescence of MSCs in vitro.[46] $CD146^+$ MSCs showed not only a more prominent capability of cartilage and bone regeneration but also a better inflammation-modulating property.[47–49] Proportion of $CD146^+$ subpopulation varies resulted from the heterogeneity of primary DPSCs.[6,50] It has been found that $CD146^+$ DPSCs promote odontogenic differentiation capabilities.[51] $CD146^+$ DPSCs were enriched on the 3D cell culture platform of hydrogel, which may be attributed to adhesion ligand density alteration of hydrogels.

The osteogenic/odontogenic differentiation of DPSCs on this 3D cell-culture platform was enhanced. One reason resulted in this finding may be that the 3D cell-culture

platform based on hydrogel provides a microenvironment with specific mechanical properties and cell adhesion ligand density that is closed to nature dental pulp tissues. On the contrary, the cell–cell/cell–matrix interaction and monolayer growth in monolayer culture is distinctive from the manner in vivo, therefore result in the relatively low level of mineralization. It should be noticed that the mRNA expression of BMP2 was significantly more highly expressed compared to other osteogenic differentiation markers in hydrogel groups, especially in the Gel-MCSs group with nearly 7 folds upregulation at 14 days. BMP2, a member of BMPs superfamily, is a ligand of TGF-β/Smad signaling pathway, which is essential for self-renewal of stem cells and able to direct osteogenic/adipogenic differentiation.[52–54] In addition, TGF-β/Smad signaling pathway sustains cross-talking with other pathways, such as phosphoinositide 3-kinase-Akt, mitogen-activated protein kinase, Wnt, Hippo and nuclear factor kB.[53] Thus, we speculate that the TGF-β/Smad signaling pathways of the cells derived from the group of hydrogels were activated and sequentially affecting other different pathways. Further studies to elucidate the definite mechanism underlined the impact of hydrogels on DPSCs are required.

In the past decades, IONPs have been widely applied in biomedicine and bioengineering such as drug delivery, imaging and cancer therapy.[15,55,56] Ferumoxytol, composed by an iron oxide core and a dextran (PSC) shell, is the only inorganic nanodrug approved by Food and Drug Administration (FDA) for clinical application in vivo.[31] Previously, we found that IONPs γ-Fe_2O_3@PSC with cellular uptake promoted the osteogenic differentiation of human bone-derived MSCs on the 2D cell culture platform.[20,57] Additionally, we previously developed a 3D culture plate for several cell lines by assembling this IONPs into hydrogels.[22,35] However, it is not unclear whether IONPs γ-Fe_2O_3@PSC retain the promotion ability of osteogenic differentiation without assembly and cellular uptake in 3D cell culture platform. The present data initially addressed this issue that revealed cellular uptake was necessary for IONPs functioned to cells and controllable assembly was preliminarily crucial to alter hydrogel mechanical property.

Conclusion

In summary, we developed a tunable hydrogel for 3D culture of DPSCs, by which DPSCs aggregated and generated spheroids with subpopulation of $CD146^+$ cells enrichment and osteogenic/odontogenic differentiation promotion. Cells derived from the DPSCs spheroids also exhibited enhanced ability for osteogenic differentiation with IONPs. Thus, this 3D cell-culture platform based on hydrogels along with IONPs may be a promising therapeutic for dentin regeneration.

Acknowledgments

This work was supported by grants from the National Key Research and Development Project (2016YFA0201704), the National Natural Science Foundation of China (81870807, 81701824, and 51832001), the China Postdoctoral Science Foundation (2017M621787), the Talent Introduction Foundation of Nanjing Medical University (2017RC07) and the Priority Academic Program Development of Jiangsu Higher Education Institutions (PAPD, 2018-87).

Disclosure

The authors report no conflicts of interest in this work.

References

1. Bernabe E, Marcenes W, Hernandez CR, et al.; Collaborators GBDOD. Global, Regional, and National Levels and Trends in Burden of Oral Conditions from 1990 to 2017: a Systematic Analysis for the Global Burden of Disease 2017 Study. *J Dent Res*. 2020;99(4):362–373. doi:10.1177/0022034520908533.
2. Peres MA, Macpherson LMD, Weyant RJ, et al. Oral diseases: a global public health challenge. *The Lancet*. 2019;394 (10194):249–260. doi:10.1016/S0140-6736(19)31146-8
3. Pitts NB, Zero DT, Marsh PD, et al. Dental caries. *Nat Rev Dis Primers*. 2017;3:17030. doi:10.1038/nrdp.2017.30
4. Moussa DG, Aparicio C. Present and future of tissue engineering scaffolds for dentin-pulp complex regeneration. *J Tissue Eng Regen Med*. 2019;13(1):58–75. doi:10.1002/term.2769
5. Bjorndal L, Simon S, Tomson PL, Duncan HF. Management of deep caries and the exposed pulp. *Int Endod J*. 2019;52(7):949–973. doi:10.1111/iej.13128
6. Gronthos S, Mankani M, Brahim J, Robey PG, Shi S. Postnatal human dental pulp stem cells (DPSCs) in vitro and in vivo. *Proc Natl Acad Sci U S A*. 2000;97(25):13625–13630. doi:10.1073/pnas.240309797
7. Nakashima M, Iohara K, Sugiyama M. Human dental pulp stem cells with highly angiogenic and neurogenic potential for possible use in pulp regeneration. *Cytokine Growth Factor Rev*. 2009;20(5–6):435–440. doi:10.1016/j.cytogfr.2009.10.012
8. Tatullo M, Marrelli M, Shakesheff KM, White LJ. Dental pulp stem cells: function, isolation and applications in regenerative medicine. *J Tissue Eng Regen Med*. 2015;9(11):1205–1216. doi:10.1002/term.1899
9. Meng H, Chowdhury TT, Gavara N. The Mechanical Interplay Between Differentiating Mesenchymal Stem Cells and Gelatin-Based Substrates Measured by Atomic Force Microscopy. *Front Cell Dev Biol*. 2021;9.
10. Vining KH, Scherba JC, Bever AM, Alexander MR, Celiz AD, Mooney DJ. Synthetic Light-Curable Polymeric Materials Provide a Supportive Niche for Dental Pulp Stem Cells. *Adv Mater*. 2018;30 (4):1704486. doi:10.1002/adma.201704486

11. Liu N, Zhou M, Zhang Q, et al. Stiffness regulates the proliferation and osteogenic/odontogenic differentiation of human dental pulp stem cells via the WNT signalling pathway. *Cell Prolif*. 2018;51(2): e12435. doi:10.1111/cpr.12435
12. Hong Chen HF, Xue W, Duan Y, et al. Regeneration of pulpo-dentinal–like complex by a group of unique multipotent CD24a+ stem cells. *Sci Adv*. 2020;6:eaay1514. doi:10.1126/sciadv.aay1514
13. Cui X, Hartanto Y, Zhang H. Advances in multicellular spheroids formation. *J R Soc Interface*. 2017;14(127):20160877. doi:10.1098/rsif.2016.0877
14. Xia Y, Sun J, Zhao L, et al. Magnetic field and nano-scaffolds with stem cells to enhance bone regeneration. *Biomaterials*. 2018;183:151–170. doi:10.1016/j.biomaterials.2018.08.040
15. Dadfar SM, Roemhild K, Drude NI, et al. Iron oxide nanoparticles: diagnostic, therapeutic and theranostic applications. *Adv Drug Deliv Rev*. 2019;138:302–325.
16. Henstock JR, Rotherham M, Rashidi H, Shakesheff KM, El Haj AJ. Remotely Activated Mechanotransduction via Magnetic Nanoparticles Promotes Mineralization Synergistically With Bone Morphogenetic Protein 2: applications for Injectable Cell Therapy. *Stem Cells Transl Med*. 2014;3(11):1363–1374. doi:10.5966/sctm.2014-0017
17. Yun HM, Kang SK, Singh RK, et al. Magnetic nanofiber scaffold-induced stimulation of odontogenesis and pro-angiogenesis of human dental pulp cells through Wnt/MAPK/NF-kappaB pathways. *Dent Mater*. 2016;32(11):1301–1311. doi:10.1016/j.dental.2016.06.016
18. Hu K, Yu T, Tang S, et al. Dual anisotropicity comprising 3D printed structures and magnetic nanoparticle assemblies: towards the promotion of mesenchymal stem cell osteogenic differentiation. *NPG Asia Materials*. 2021;13(1). doi:10.1038/s41427-021-00288-x.
19. Shuai C, Yang W, He C, et al. A magnetic micro-environment in scaffolds for stimulating bone regeneration. *Mater Des*. 2020;185.
20. Wang Q, Chen B, Ma F, et al. Magnetic iron oxide nanoparticles accelerate osteogenic differentiation of mesenchymal stem cells via modulation of long noncoding RNA INZEB2. *Nano Res*. 2016;10(2):626–642. doi:10.1007/s12274-016-1322-4
21. Huang Q, Zou Y, Arno MC, et al. Hydrogel scaffolds for differentiation of adipose-derived stem cells. *Chem Soc Rev*. 2017;46(20):6255–6275. doi:10.1039/C6CS00052E
22. Hu K, Sun J, Guo Z, et al. A novel magnetic hydrogel with aligned magnetic colloidal assemblies showing controllable enhancement of magnetothermal effect in the presence of alternating magnetic field. *Adv Mater*. 2015;27(15):2507–2514. doi:10.1002/adma.201405757
23. Xue K, Wang X, Yong PW, et al. Hydrogels as Emerging Materials for Translational Biomedicine. *Advanced Therapeutics*. 2019;2(1):1800088. doi:10.1002/adtp.201800088
24. Zhang M, Yan S, Xu X, et al. Three-dimensional cell-culture platform based on hydrogel with tunable microenvironmental properties to improve insulin-secreting function of MIN6 cells. *Biomaterials*. 2021;270:120687. doi:10.1016/j.biomaterials.2021.120687
25. Tang SJ, Hu K, Sun JF, et al. High Quality Multicellular Tumor Spheroid Induction Platform Based on Anisotropic Magnetic Hydrogel. *ACS Appl Mater Interfaces*. 2017;9(12):10446–10452. doi:10.1021/acsami.6b15918
26. Yu TT, Hu K, Xu QF, et al. An Easy-to-Fabricate Hydrogel Platform with Tunable Stiffness and Cell Anchorage: validation of Its Feasibility in Modulating Sonic Hedgehog Signaling Pathway Physically. *Macromol Mater Eng*. 2020;305(4):1900759. doi:10.1002/mame.201900759
27. Yu T, Hu Y, Feng G, Hu K, Graphene-Based Flexible A. Device as a Specific Far-Infrared Emitter for Noninvasive Tumor Therapy. *Advanced Therapeutics*. 2020;3(3):1900195. doi:10.1002/adtp.201900195
28. Lew WZ, Feng SW, Lin CT, Huang HM. Use of 0.4-Tesla static magnetic field to promote reparative dentine formation of dental pulp stem cells through activation of p38 MAPK signalling pathway. *Int Endod J*. 2019;52(1):28–43. doi:10.1111/iej.12962
29. Lew WZ, Huang YC, Huang KY, Lin CT, Tsai MT, Huang HM. Static magnetic fields enhance dental pulp stem cell proliferation by activating the p38 mitogen-activated protein kinase pathway as its putative mechanism. *J Tissue Eng Regen Med*. 2018;12(1):19–29. doi:10.1002/term.2333
30. Luo L, He Y, Wang X, et al. Potential Roles of Dental Pulp Stem Cells in Neural Regeneration and Repair. *Stem Cells Int*. 2018;2018:1731289. doi:10.1155/2018/1731289
31. Chen B, Sun J, Fan F, et al. Ferumoxytol of ultrahigh magnetization produced by hydrocooling and magnetically internal heating co-precipitation. *Nanoscale*. 2018;10(16):7369–7376. doi:10.1039/C8NR00736E
32. Vining KH, Mooney DJ. Mechanical forces direct stem cell behaviour in development and regeneration. *Nat Rev Mol Cell Biol*. 2017;18(12):728–742. doi:10.1038/nrm.2017.108
33. Bellas E, Chen CS. Forms, forces, and stem cell fate. *Curr Opin Cell Biol*. 2014;31:92–97. doi:10.1016/j.ceb.2014.09.006
34. Fennema E, Rivron N, Rouwkema J, van Blitterswijk C, de Boer J. Spheroid culture as a tool for creating 3D complex tissues. *Trends Biotechnol*. 2013;31(2):108–115. doi:10.1016/j.tibtech.2012.12.003
35. Hu K, Zhou N, Li Y, et al. Sliced Magnetic Polyacrylamide Hydrogel with Cell-Adhesive Microarray Interface: a Novel Multicellular Spheroid Culturing Platform. *ACS Appl Mater Interfaces*. 2016;8(24):15113–15119. doi:10.1021/acsami.6b04112
36. Huang D, Huang Y, Xiao Y, et al. Viscoelasticity in natural tissues and engineered scaffolds for tissue reconstruction. *Acta Biomater*. 2019;97:74–92. doi:10.1016/j.actbio.2019.08.013
37. Grolman JM, Weinand P, Mooney DJ. Extracellular matrix plasticity as a driver of cell spreading. *Proc Natl Acad Sci U S A*. 2020;117(42):25999–26007. doi:10.1073/pnas.2008801117
38. Chaudhuri O, Cooper-White J, Janmey PA, Mooney DJ, Shenoy VB. Effects of extracellular matrix viscoelasticity on cellular behaviour. *Nature*. 2020;584(7822):535–546. doi:10.1038/s41586-020-2612-2
39. Xia J, Zhang H, Gao X, et al. E-cadherin-mediated contact of endothelial progenitor cells with mesenchymal stem cells through beta-catenin signaling. *Cell Biol Int*. 2016;40(4):407–418. doi:10.1002/cbin.10579
40. Cao L, Zhang Y, Qian M, et al. Construction of multicellular aggregate by E-cadherin coated microparticles enhancing the hepatic specific differentiation of mesenchymal stem cells. *Acta Biomater*. 2019;95:382–394. doi:10.1016/j.actbio.2019.01.030
41. Hawkins K, Mohamet L, Ritson S, Merry CL, Ward CM. E-cadherin and, in its absence, N-cadherin promotes Nanog expression in mouse embryonic stem cells via STAT3 phosphorylation. *Stem Cells*. 2012;30(9):1842–1851. doi:10.1002/stem.1148
42. Cosgrove BD, Mui KL, Driscoll TP, et al. N-cadherin adhesive interactions modulate matrix mechanosensing and fate commitment of mesenchymal stem cells. *Nat Mater*. 2016;15(12):1297–1306. doi:10.1038/nmat4725
43. Wang Z, Yan X. CD146, a multi-functional molecule beyond adhesion. *Cancer Lett*. 2013;330(2):150–162. doi:10.1016/j.canlet.2012.11.049
44. Ye Z, Zhang C, Tu T, et al. Wnt5a uses CD146 as a receptor to regulate cell motility and convergent extension. *Nat Commun*. 2013;4(1):2803. doi:10.1038/ncomms3803
45. Yawata T, Higashi Y, Kawanishi Y, et al. CD146 is highly expressed in glioma stem cells and acts as a cell cycle regulator. *J Neurooncol*. 2019;144(1):21–32. doi:10.1007/s11060-019-03200-4

46. Yang YK, Ogando CR, Wang See C, Chang TY, Barabino GA. Changes in phenotype and differentiation potential of human mesenchymal stem cells aging in vitro. *Stem Cell Res Ther*. 2018;9(1):131. doi:10.1186/s13287-018-0876-3
47. Li X, Guo W, Zha K, et al. Enrichment of CD146(+) Adipose-Derived Stem Cells in Combination with Articular Cartilage Extracellular Matrix Scaffold Promotes Cartilage Regeneration. *Theranostics*. 2019;9(17):5105–5121. doi:10.7150/thno.33904
48. Wang Y, Xu J, Chang L, et al. Relative contributions of adipose-resident CD146(+) pericytes and CD34(+) adventitial progenitor cells in bone tissue engineering. *NPJ Regen Med*. 2019;4:1. doi:10.1038/s41536-018-0063-2
49. Jin SS, He DQ, Luo D, et al. A Biomimetic Hierarchical Nanointerface Orchestrates Macrophage Polarization and Mesenchymal Stem Cell Recruitment To Promote Endogenous Bone Regeneration. *ACS Nano*. 2019;13(6):6581–6595. doi:10.1021/acsnano.9b00489
50. Sharpe PT. Dental mesenchymal stem cells. *Development*. 2016;143(13):2273–2280. doi:10.1242/dev.134189
51. Matsui M, Kobayashi T, Tsutsui TW. CD146 positive human dental pulp stem cells promote regeneration of dentin/pulp-like structures. *Hum Cell*. 2018;31(2):127–138. doi:10.1007/s13577-017-0198-2
52. Salazar VS, Gamer LW, Rosen V. BMP signalling in skeletal development, disease and repair. *Nat Rev Endocrinol*. 2016;12(4):203–221. doi:10.1038/nrendo.2016.12
53. Luo K. Signaling Cross Talk between TGF-beta/Smad and Other Signaling Pathways. *Cold Spring Harb Perspect Biol*. 2017;9(1):a022137. doi:10.1101/cshperspect.a022137
54. Li S-N, Wu J-F. TGF-β/SMAD signaling regulation of mesenchymal stem cells in adipocyte commitment. *Stem Cell Res Ther*. 2020;11(1):41. doi:10.1186/s13287-020-1552-y
55. Zhu L, Zhou Z, Mao H, Yang L. Magnetic nanoparticles for precision oncology: theranostic magnetic iron oxide nanoparticles for image-guided and targeted cancer therapy. *Nanomedicine*. 2017;12(1):73–87. doi:10.2217/nnm-2016-0316
56. Oleksa V, Bernátová I, Patsula V, et al. Poly(ethylene glycol)-Alendronate-Coated Magnetite Nanoparticles Do Not Alter Cardiovascular Functions and Red Blood Cells' Properties in Hypertensive Rats. *Nanomaterials*. 2021;11(5):1238. doi:10.3390/nano11051238
57. Wang Q, Chen B, Cao M, et al. Response of MAPK pathway to iron oxide nanoparticles in vitro treatment promotes osteogenic differentiation of hBMSCs. *Biomaterials*. 2016;86:11–20. doi:10.1016/j.biomaterials.2016.02.004